



An energy-isochronous multi-pass time-of-flight mass spectrometer consisting of two coaxial electrostatic mirrors

H. Wollnik*, A. Casares

II. Physikalisches Institut, Justus-Liebig-Universität, H-Buff-Ring 16, D-1635392 Giessen, Germany

Received 27 December 2002; accepted 24 February 2003

Abstract

Energy-isochronous time-of-flight mass spectrometers can achieve high mass resolving powers by using the same flight pass repeatedly and thus obtaining long overall flight distances. If such systems must achieve high transmission in addition to their isochronicity, they must be designed such that their lateral phase-space acceptance is larger than the corresponding emittance of the injected ion beam. It furthermore is advantageous to construct the system from matched unit cells, a technique also used in the design of accelerator storage rings. One such time-of-flight mass spectrometer has been built as a system in which ions are repeatedly reflected between two grid-free ion mirrors whose optic axes coincide. For a 0.4 m long system, through which ions were reflected 101 times, mass resolving powers of $m/\Delta m \geq 18,000$ have been achieved with a transmission of about 40%. © 2003 Elsevier Science B.V. All rights reserved.

Keywords: Time-of-flight mass spectrometer; Mass measurements; Mass accuracy

1. Introduction

In order to obtain high mass resolving power in a time-of-flight mass spectrometer (TOF-MS) the ion pulses must be short compared to the overall flight time. Since the ion pulses cannot be shortened below certain limits, a high-performance system must either be very large or must use the geometrically available flight distance repeatedly. Such multi-pass time-of-flight mass spectrometers (MTOF-MS) can be built as low-energy storage rings [1] or as linear devices in which the ions are reflected back and forth between mirrors [2]. In one such system we have

achieved [3] high mass resolving powers for 1500 eV ions in a system that consisted of one static and two small switchable grid-free ion mirrors. For these measurements we have used ion pulses that were a few nanoseconds long, formed by a klystron-like bunching action exerted on ions produced continuously in an electron impact ion source as described in Refs. [4,5].

The overall transmission in this system was limited, however, by image aberrations. These aberrations produced a beam halo, which was not fully transmitted because of the limited apertures of some electrodes. Such losses are considerably reduced in the mirror arrangement described here and shown in Fig. 1. This system is characterized by considerably reduced image aberrations since it consists of only two switchable grid-free ion mirrors, both consisting of rotationally symmetric coaxially arranged electrodes.

* Corresponding author. Tel.: +49-641-99-33246;
fax: +49-641-99-33239.
E-mail address: h.wollmik@uni-giessen.de (H. Wollnik).

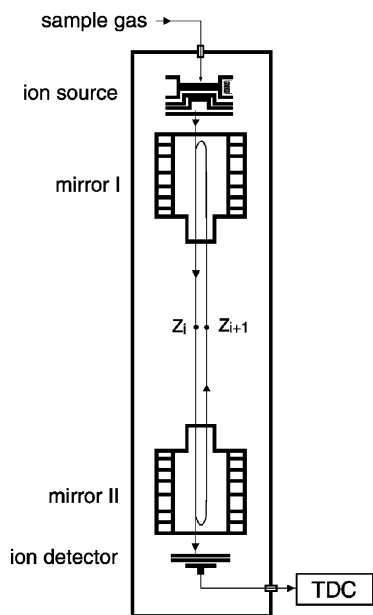


Fig. 1. Principle of a coaxial multi-pass time-of-flight mass spectrometer (MTOF-MS). The positions z_i and z_{i+1} should almost coincide ideally.

2. Ion-optical considerations for a coaxial MTOF-MS

The ion-optical properties of a MTOF-MS can be described as a multitude of identical cells, if the direction of the optic axis is reversed after every reflection. A reference ion of mass-to-charge ratio (m_0/q_0) and energy-to-charge ratio (K_0/q_0) can move along this optic axis, which we will refer to as the z -axis. By starting such a reference particle simultaneously with an arbitrary ion of mass-to-charge ratio $(m_0/q_0)(1 + \delta_m)$ and an energy-to-charge ratio $(K_0/q_0)(1 + \delta_K)$, one can describe how the motions of these two particles differ transversally as well as longitudinally at a certain z -position, i.e., perpendicular as well as parallel to the optic axis.

Since the MTOF-MS under consideration here consists only of coaxial rotationally symmetric electrodes, it is advantageous to postulate the optic axis to coincide with the electrode axis and to describe the trajectory of an arbitrary ion only by its transverse

deviation $x(z)$ and its transverse inclination $a(z) = p_x(z)/p_0(z)$ relative to the optic axis. At the position z here, $p_0(z)$ describes the ion's full momentum and $p_x(z)$ its x -component, i.e., the component perpendicular to the optic axis. The longitudinal deviation of this arbitrary ion from a reference ion that started simultaneously will be described as the difference $\Delta t(z)$ between the times when these two particles pass a certain z -position. Assuming that there are $2N$ characteristic positions along the z -axis, one can characterize an arbitrary ion by: $x(z_i)$, $a(z_i)$, $\Delta t(z_n)$ with $i = 0, 1, 2, \dots, 2N$.

Knowing $x(z_i)$, $a(z_i)$ at a position z_i one thus can determine $x(z_{i+1})$, $a(z_{i+1})$ at a position z_{i+1} . To first order these relations read:

$$x(z_{i+1}) = (x_{i+1}|x_i)x(z_i) + (x_{i+1}|a_i)a(z_i) + (x_{i+1}|K)\delta_K(z_i) + \dots \quad (1a)$$

$$a(z_{i+1}) = (a_{i+1}|x_i)x(z_i) + (a_{i+1}|a_i)a(z_i) + (a_{i+1}|K)\delta_K(z_i) + \dots \quad (1b)$$

$$\Delta t(z_{i+1}) = (t_{i+1}|x_i)x(z_i) + (t_{i+1}|a_i)a(z_i) + (t_{i+1}|K)\delta_K(z_i) + (t_{i+1}|m)_{i+1}\delta_m + \dots \quad (1c)$$

with $\delta_K(z_n) = [K(z_i) - K_0(z_i)]/K_0(z_i)$ at the position z_i . Because of the symplectic condition, there are relations [6] between the coefficients of Eq. (1):

$$(x_{i+1}|x_i)(x_{i+1}|a_i) - (a_{i+1}|x_i)(a_{i+1}|a_i) = 1 \quad (2a)$$

$$(x_{i+1}|x_i)(a_{i+1}|K) - (a_{i+1}|x_i)(x_{i+1}|K) = \left(\frac{v_0}{2}\right)(t_{i+1}|a_i) \quad (2b)$$

$$(x_{i+1}|a_i)(a_{i+1}|K) - (a_{i+1}|a_i)(x_{i+1}|K) = \left(\frac{v_0}{2}\right)(t_{i+1}|x_i) \quad (2c)$$

Since the optic axis of the system under investigation here is straight (see Fig. 1), the system is energy achromatic to first order [6], i.e., an ion whose energy-to-charge ratio $(K_0/q_0)(1 + \delta_K)$ deviates from that of a reference ion, is not deflected from the z -axis which postulates $(x_{i+1}|K) = (a_{i+1}|K) = 0$. Thus, for

first order the Eqs. (1) and (2) simplify to:

$$x(z_{i+1}) = (x_{i+1}|x_i)x(z_i) + (x_{i+1}|a_i)a(z_i) + \dots \quad (3a)$$

$$a(z_{i+1}) = (a_{i+1}|x_i)x(z_i) + (a_{i+1}|a_i)a(z_i) + \dots \quad (3b)$$

$$\Delta t(z_{n+1}) = (t_{n+1}|K)\delta_K(z_n) + (t_{n+1}|m)\delta_m + \dots \quad (3c)$$

with the side condition of Eq. (2a) that allows determination of one coefficient of Eqs. (3a) and (3b) from the other three. Note here that the indices in Eqs. (3a)–(3c) are chosen to be different which indicate that the z_i and z_{i+1} may be chosen differently from the z_n and z_{n+1} . This is often advantageous since Eqs. (3a) and (3b) control the transverse motion of ions through an MTOF-MS, i.e., they control the ion transmission, while Eq. (3c) controls the achievable time-of-flight mass resolving power $1/\delta_m$ and energy resolving power $1/\delta_K$.

If the ion flight time from z_n to z_{n+1} must characterize the ion's mass-to-charge ratio, the system should be designed such that the flight time of a reference ion of energy-to-charge ratio K_0/q_0 is identical to the flight time of an arbitrary ion of equal mass but different energy-to-charge ratio $K_0(1 + \delta_K)$ with $\delta_K \neq 0$, or in other words, such that $(t_{n+1}|K) = 0$ in Eq. (3c). A system for which this relation holds is said to be energy-isochronous. Physically, this condition can be fulfilled by sending ions of higher energy $K_0\delta_K \geq K_0$ on a detour as compared to reference ions of energy K_0 . In an MTOF-MS, as indicated in Fig. 1, this can be achieved by choosing the repeller field strength in the ion mirrors appropriately so that more energetic ions penetrate an appropriate distance deeper into the ion mirrors [6,7]. Though this condition of isochronicity must only be fulfilled between the positions from where the ions start and where they are detected, there are advantages in designing the MTOF-MS such that many intermediate isochronous points exist, as is the case for the system of Fig. 1.

To voltages that had to be supplied to the different electrodes of the ion mirrors, i.e., the coefficients of Eq. (1), were determined [8] from SIMION [9] ray tracing calculations. For these calculations a beam of 1500 eV ions was assumed that filled a phase-space volume of $\varepsilon_x \approx 25\pi$ mm mrad since this was the

phase-space area to which apertures limited the ion beam in our finally built MTOF-MS.

2.1. Transverse first-order properties of a coaxial MTOF-MS

To achieve optimal conditions for a multitude of ion reflections in a system that consists of two identical ion mirrors—as shown in Fig. 1—it is advantageous to start all considerations from that z -position that is exactly at the midpoint between the two ion mirrors, $z = z_{\text{mid}}$. The optical properties of the two ion mirrors then should be chosen such that the transverse envelope of the ion beam reproduces itself after every reflection, i.e., whenever the ion beam passes the midpoint between the ion mirrors. This situation is also described by stating that all ion trajectories that were parallel to the z -axis at this midpoint are focused to a point on the z -axis again after the reflection. Such a system is known as a waist-to-waist transforming unit cell [6].

In such a system one finds that an ion beam that initially fills an upright phase-space ellipse at the midpoint $z = z_{\text{mid}}$ between the mirrors will do this again after every reflection, i.e., when it again reaches the position $z = z_{\text{mid}}$. Such a postulate can be fulfilled by the ion mirror under consideration if $(x_{i+1}|x) = (a_{i+1}|a) = 0$ in Eqs. (3a) and (3b). Thus, there are only two non-vanishing coefficients remaining, i.e., $(x_{i+1}|a)$ and $(a_{i+1}|x)$. However, because of Eq. (2a) there is actually only one, i.e., $(x_{i+1}|a) = -(a_{i+1}|x)^{-1}$, whose magnitude should be chosen such that $(x_{i+1}|a)$ equals the ratio between the maximal $x(z_{\text{mid}})$ and the maximum $a(z_{\text{mid}})$ of the initial ion beam. This can be expressed as

$$(x_{i+1}|a_i) = \frac{x_{\text{max}}(z_{\text{mid}})}{a_{\text{max}}(z_{\text{mid}})} \quad (4)$$

with $i = 1, 2, \dots, 2N - 1$ and all z_i coinciding physically at the position z_{mid} , i.e., at the midpoint between the two ion mirrors. Here, it is assumed that the ions pass N times through the full MTOF-MS, so that the reference ions pass through a flight path of length

$$\ell_{\text{total}} = N(\ell_{R1} + \ell_{R2}) + \ell_{SD} \quad (5)$$

where ℓ_{SD} is the distance between the ion source and the ion detector in Fig. 1; ℓ_{R2} is the length of the flight path from z_{mid} the midpoint between the ion mirrors through ion mirror I and back to z_{mid} ; ℓ_{R1} is the length of the flight path from z_{mid} the midpoint between the ion mirrors through ion mirror II and back to z_{mid} with ℓ_{R1} and ℓ_{R2} not necessarily being equal. However, we chose $\ell_{R1} = \ell_{R2}$ for our system. To experimentally fulfill Eq. (4) in a straight-forward fashion, we have provided electrostatic Einzel-lenses of variable strengths adjacent to both ion mirrors, i.e., in that part of each ion mirror that faces the other mirror. These Einzel-lenses are formed by applying appropriate potentials to the last electrodes of each ion mirror so that a potential distribution along the beam axis of each of the ion mirrors is obtained that is similar to that shown in Fig. 2.

Since the ions start at the bunching position z_0 close to the ion source and not at z_{mid} , they first need to be transported from z_0 to z_{mid} before they can start their multi-cell passage from z_i to z_{i+1} with $i = 1, 2, \dots, 2N$.

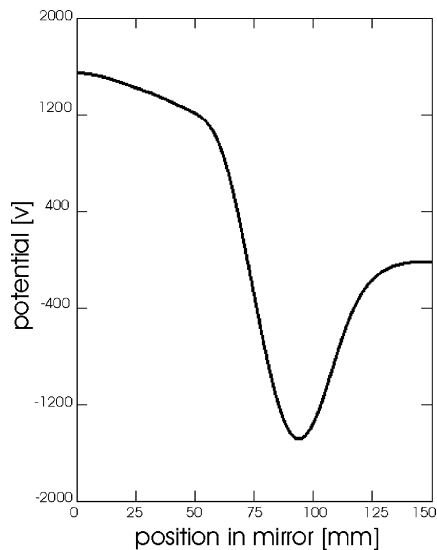


Fig. 2. The calculated potential along the optic axis of one of the ion mirrors formed by ring electrodes at different potentials as realized in the here described MTOF-MS. Note that the first ≈ 60 mm constitutes a mirror and the second ≈ 60 mm an accelerating Einzel-lens, the center electrode of which is 26 mm long while the lengths of the other ring electrodes were only 8 mm.

This requires the potentials on the electrodes of ion mirror I to be changed for a short time at the beginning of the measurement cycle, such that the bunched cloud of ions can pass into the region between the mirrors. During this time the potential distribution in the mirror is chosen such that the ion cloud will fill a transverse phase-space volume that is approximately upright once it reaches the position z_{mid} . Analogously, the potentials on the ion mirror II must be changed for a short time when the ions have performed the required N passes through the full system, so that they can be recorded in the ion detector (see Fig. 1).

2.2. Longitudinal first-order properties of the coaxial MTOF-MS

While for the transverse optical properties the path length of one full cell is exactly $\Delta\ell_{transverse} = \ell_{R1} + \ell_{R2}$, we have chosen the length of one full cell for the longitudinal properties to be $\Delta\ell_{longit} = (\ell_{R1} + \ell_{R2}) + \ell_{SD}/N$ so that the total flight distance $N(\ell_{R1} + \ell_{R2}) + \ell_{SD}$ is divided into N equally long sub-cells. Thus, z_{n+1} is always downstream of z_{i+1} while $z_n=0$ is at the bunching position of the ion source and $z_n=2N$ is at the position of the ion detector. Note, however, that the flight times through the first and the last cell of the system differ from the flight times through the others since in these cells the ions must pass through the switched-down ion mirrors.

3. The design of the coaxial MTOF-MS

The MTOF-MS was built as shown in Fig. 1. The two ion mirrors each consisted of seven-ring electrodes of 40 mm inner diameter. Of these seven electrodes six were 8 mm long and one 26 mm. This longer electrode has the biggest influence on the focal length of the mentioned lens in Fig. 2 and is the second to last electrode in each ion mirror. These electrodes were closely adjacent since they all were separated from their neighbors by 75 μm thick Capton foils. These ion mirrors were salvaged from the experiment described in Ref. [3]. Only the mounting of the mirrors was changed so

that at the end the axes of the two identical ion mirrors coincided as is postulated in Fig. 1. The overall system length is 420 mm and the path length from z_i to z_{i+1} is $(\ell_{R1} + \ell_{R2})/2 \approx 300$ mm. The ring electrodes were all grid-free except for the final reflecting electrodes. In mirror I this grid is located at the side that faces the ion source while in mirror II this grid is located at the side that faces the ion detector. During the multi-pass operation, the potentials V_1 of these grids were so high that the 1500 eV ions turned around about 1.5 mm before these grids. Only during entrance into and exit out of the multi-pass system were the potentials of the gridded electrodes lowered to about half of their nominal values for $\approx 3 \mu\text{s}$. During these short periods, the ions traversed these grids, causing intensity losses of $\approx 10\%$. These losses, however, were independent of the number of reflections in the MTOF-MS.

This lowering of the potentials on the back electrodes of the ion mirrors for $\approx 3 \mu\text{s}$ required fast high-voltage pulsers. These pulsers were integrated with precision DC-voltage supplies that also fed proper potentials to the different mirror electrodes through temperature-controlled resistive voltage dividers. In

order to limit the pulse power, we reduced the capacitance between the pulsed electrodes to values below ≈ 50 pF. For the same reason, we used push-pull pulser circuits that merely transport electric charges from one capacitor to another.

4. Tests of the coaxial MTOF-MS

To test the MTOF-MS we have passed the ions up to 101 times through the $\ell_{R1} = \ell_{R2} \approx \ell_{SD} \approx 300$ mm flight path of one passage, with the initial kinetic energies of the ions being 1500 eV. For ions of the CO–N₂ mass doublet the overall flight time for this ≈ 30 m path was $\approx 380 \mu\text{s}$ as one may take from Fig. 3 with a flight time difference between the CO and N₂ ions being $\Delta t \approx 75$ ns. This Δt corresponds to their mass difference which is $\approx 28.00611 - 27.99491$ u, i.e., ≈ 0.0112 u or ≈ 10.44 MeV. The FWHM peak width here is $\Delta t \leq 12$ ns, i.e., $\leq 15\%$ of 75 ns. Thus, one finds that the FWHM time-of-flight resolving power is $T_0/\Delta T \geq 380,000/12 \geq 32,000$ and the FWHM mass resolving power is $m_0/\Delta m \geq 16,000$ with the

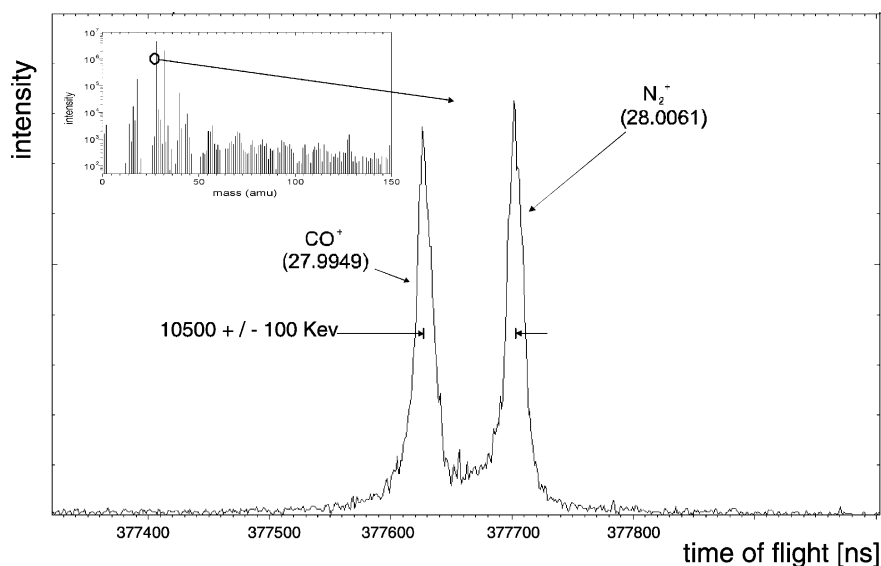


Fig. 3. The mass spectrum of CO-enriched ambient air, showing the N₂–CO mass-doublet at $m_0 \approx 28$ u or $m_0 \approx 26,100$ MeV as recorded after 101 passes in the coaxial MTOF-MS of ≈ 300 mm flight path per passage. From this spectrum one determines the known mass difference $\Delta m \approx 0.0112$ u or $\Delta m \approx 10.5$ MeV with an FWHM peak width Δm of 15% of Δm and a corresponding mass accuracy of $\leq 0.1 \times 0.15 \Delta m/m_0 \leq 10$ ppm. Here, it is assumed that one can determine the centroid of each mass line to $\leq 10\%$ of Δm .

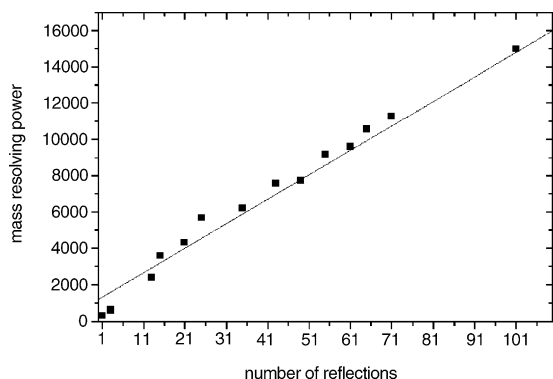


Fig. 4. The mass resolving power $m/\Delta m$ for the coaxial MTOF-MS as function of the number of reflections.

best value obtained being $\approx 18,000$. With the achieved statistics the center of gravity of each mass line could be determined to $\leq 10\%$ of ΔT and thus to ≈ 1.0 ns or $\leq (1.0/75) \times 10.44 \leq 0.17$ MeV.

To demonstrate how the mass resolving power and the ion transmission of the system varied with the number of reflections of ions, we performed a series of experiments, the results of which are shown in Figs. 4 and 5. The large scatter in the data is due to the fact that each point had to be measured in a separate experiment, which required a new adjustment of several potentials.

The achieved mass resolving power $m/\Delta m$ as shown in Fig. 4 increases linearly with the number of

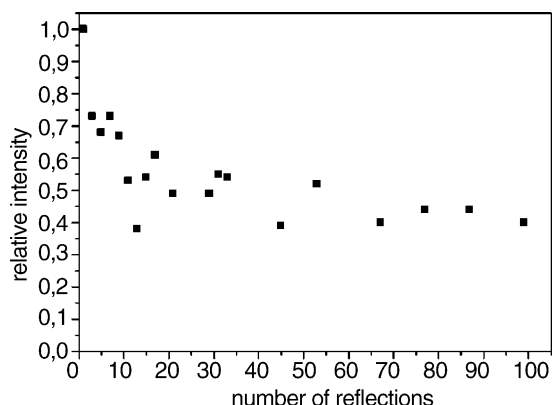


Fig. 5. The transmission for the coaxial MTOF-MS as function of the number of reflections.

reflections in the MTOF-MS to values $\geq 16,000$. Even better values were reported in Refs. [3,10], however, differently than in the systems of these reports the ion transmission (see Fig. 5) is more or less independent of the number of reflections in the new MTOF-MS. The transmitted ion intensity as plotted in Fig. 5 was determined relative to the intensity recorded in the ion detector, when all electrodes of the ion mirror—but not those of the main lenses, i.e., the three electrodes of each electrode stack (see Fig. 1) that face the other—were grounded. Overall, there is an initial $\approx 50\%$ loss of the recorded ion intensity. This loss occurs when the ion beam enters the ion-optical system of the MTOF-MS, while even after many reflections $\approx 40\%$ of the initial ion intensity remains. This result we regard as a major improvement of the new system over the one of Ref. [3] since it allows the number of reflections to be increased to very large values.

Acknowledgements

We gratefully acknowledge financial support from the “German Ministry für Bildung und Wissenschaft” and the Max-Planck-Institut für Aeronomie in Lindau, Germany.

References

- [1] H. Wollnik, *Nucl. Instrum Methods* B26 (1987) 267.
- [2] H. Wollnik, M. Przewłoka, *Int. J. Mass Spectrom. Ion Processes* 96 (1990) 267.
- [3] H. Wollnik, A. Casares, A. Kholomeev, *Int. J. Mass Spectrom.* 206 (2001) 267.
- [4] H. Wollnik, in: A. Benninghoven (Ed.), *Ion Formation from Organic Solids*, Springer Proceedings in Physics, vol. 9, 1986, p. 184.
- [5] R. Grix, U. Grüner, G. Li, H. Stroh, H. Wollnik, *Int. J. Mass Spectrom. Ion Processes* 93 (1988) 323.
- [6] H. Wollnik, *Optics of Charged Particles*, Academic Press, Orlando, 1987.
- [7] B.A. Mamyrin, V.I. Karataev, D.V. Shmikk, A. Zagulin, *JETP* 37 (1973) 45.
- [8] A. Casares, Thesis, University Giessen, Germany, 2001.
- [9] D.A. Dahl, *Int. J. Mass Spectrom.* 200 (2000) 3.
- [10] S.K.G. Piyadasa, P. Haakenson, T.R. Ariyaratne, *Rapid Commun. Mass Spectrom.* 13 (1999) 620.